Canadian Mineralogist
Vol. 24, pp. 605-614 (1986)

THE CRYSTAL STRUCTURE OF BOBFERGUSONITE

T. SCOTT ERCIT[1], FRANK C. HAWTHORNE AND PETR ČERNÝ
Department of Geological Sciences, University of Manitoba, Winnipeg, Manitoba R3T 2N2

ABSTRACT

Bobfergusonite $Na_2Mn_5Fe^{3+}Al(PO_4)_6$ is monoclinic, $P2_1/n$, with a 12.776(2), b 12.488(2), c 11.035(2) Å, β 97.21(1)°, V 1746.7(4) Å^3, $Z=4$. The crystal structure, a more highly ordered derivative of the wyllieite structure, was refined on the basis of a transformed wyllieite structure, resulting in an R index of 3.8 % for 2889 observed (3σ) reflections measured on a single crystal of red-brown holotype material. The structure of bobfergusonite is topologically identical to that of wyllieite and alluaudite, but differs from both these structure types in terms of its M-cation ordering. It is a layer structure, and has alternations of two types of layer along Y. One type of layer consists of M-cation (Mn,Fe^{3+}, Al) octahedral chains cross-linked by phosphate tetrahedra. Each chain has *intrachain* M^{3+}–M^{2+} ordering similar to that of the wyllieite structure; however, unlike both the wyllieite and alluaudite structures, *interchain* ordering of Al and Fe^{3+} occurs, resulting in two compositions of chain. The second layer of the structure is identical to its counterpart in the wylliete structure, and consists of two types of chains of X-cation (Na, Mn) polyhedra that run parallel to X. One chain consists of alternating, face-sharing Na and Mn polyhedra; the other consists exclusively of edge-sharing Na polyhedra. These two types of chains are not cross-linked within the layer, and serve to link the layers of M-cation chains and PO_4 tetrahedra.

Keywords: bobfergusonite, crystal structure, phosphate, wyllieite, alluaudite, cation ordering.

SOMMAIRE

La bobfergusonite $Na_2Mn_5Fe^{3+}Al(PO_4)_6$ est monoclinique, $P2_1/n$, a 12.776(2), b 12.488(2), c 11.035(2) Å, β 97.21(1)°, V 1746.7(4) Å^3, $Z=4$. C'est un dérivé mieux ordonné du type structural de la wyllieite que l'on a affiné sur un modèle transformé de cette structure. L'affinement a donné un résidu R de 3.8% pour 2889 réflexions observées (3σ) sur cristal unique du holotype rouge-brun. La structure est topologiquement identique à celles de la wyllieite et de l'alluaudite, mais diffère de à celles-ci dans le degré d'ordre des cations M. La structure contient deux sortes de feuillets en alternance le long de Y. Dans un des feuillets, des chaînes d'octaèdres de cations M (Mn,Fe^{3+}, Al) sont entre-liées par des tétraèdres de phosphate. A l'intérieur d'une chaîne, la mise en ordre des cations M^{3+}–M^{2+} ressemble à ce que l'on trouve dans la wyllieite; contrairement aux structures de la wyllieite et de l'alluaudite, cependant, Al et Fe^{3+} sont ordonnés entre les chaînes, ce qui donne deux chaînes distinctes en composition. Le deuxième feuillet, identique à son analogue dans la wyllieite, contient deux types de chaîne de polyèdres à cations X (Na,Mn) parallèles à X. Une chaîne contient une alternance de polyèdres à Na et Mn à faces partagées; l'autre contient exclusivement des polyèdres à Na à arêtes partagés. Ces deux sortes de chaîne, qui ne sont pas entre-liées dans le feuillet, lient les feuillets de polyèdres à cations M aux tétraèdres PO_4.

(Traduit par la Rédaction)

Mots-clés: bobfergusonite, structure cristalline, phosphate, wyllieite, alluaudite, mise en ordre des cations.

INTRODUCTION

Bobfergusonite $Na_2Mn_5Fe^{3+}Al(PO_4)_6$ was discovered by Ercit *et al.* (1986) in granitic pegmatites of the Cross Lake area, Manitoba. The mineral is closely related to wyllieite-group and alluaudite-group minerals, yet differs from all known members of these groups both in chemistry and structure. The chemistry, X-ray crystallography and optical and physical properties of the mineral are described in Ercit *et al.* (1986). Because of the close relationship of bobfergusonite to the wyllieite-group and alluaudite-group minerals, it was necessary to determine the structure of the mineral as part of its characterization as a new species.

EXPERIMENTAL

A cleavage fragment measuring 0.18 × 0.29 × 0.29 mm along its edges was used for data collection. The fragment was selected from red-brown holotype material (P–1 of Ercit *et al.* 1986). Precession photographs confirmed the identity of the fragment as bobfergusonite and indicated it to be well crystallized and single. Intensity data were collected with a Nicolet R3m automated four-circle diffractometer operating at 50 kV and 35 mA, using graphite-monochromated Mo$K\alpha$ radiation. Unit-cell parameters for the crystal (Table 1) were refined from a subset of 25 intense diffraction-maxima used in centring the crystal. A 2θ:θ scanning mode was used to collect the intensity data. Each scan covered a range of 2° 2θ plus the α_1–α_2 separation, in 96 steps. Scanning speeds were variable, ranging from 4°/min for weak diffractions to 29.3°/min for in-

[1]Present address: Mineral Sciences Division, National Museum of Natural Sciences, Ottawa, Ontario K1A 0M8.

TABLE 1. MISCELLANEOUS INFORMATION FOR BOBFERGUSONITE

a	12.776(2) Å		Space group		$P2_1/n$
b	12.488(2)		Crystal size		0.18x0.29x0.29 mm
c	11.035(2)		μ, Radiation		44.5 cm^{-1}, MoKα
β	97.21(1)°		Total Fo, Obs. Fo		4204, 2889
V	1746.7(4) Å^3		Final R, wR		3.8, 3.4 %

Cell Contents (Z=4):
$Na_{2.06}Mn_{4.21}Fe^{2+}_{.04}Fe^{3+}_{.79}Al_{1.38}Ca_{4.9}Mg_{.09}Zn_{.05}P_6O_{23.75}OH_{.25}$*

$R = \Sigma(|Fo|-|Fc|)\ /\Sigma|Fo|$
$wR = [\Sigma w(|Fo|-|Fc|)^2\ /\Sigma w|Fo|^2]^{\frac{1}{2}}$, w=1

* OH:O calculated for charge balance

tense diffractions, and were adjusted automatically. Backgrounds were measured for half the scan time at the beginning and end of each scan. Three standard reflections were monitored every 45 reflections for changes in beam intensity or crystal orientation. All such changes were insignificant. Data were collected over 1 asymmetric unit of reciprocal space, initially to $\sin\theta/\lambda = 0.7035$, but later only to $\sin\theta/\lambda = 0.5946$, to reduce the number of data. In all, 4204 reflections were collected, of which 2889 were considered observed ($I > 3\sigma$).

Subsequent to the collection of the main data-set, additional intensity-data were collected on 11 strong diffraction-maxima evenly dispersed over a range of 6 to 53°2θ. These data were collected every 10° while rotating each reflection 360° about its diffraction vector (ψ), using the same set of scan parameters as the main collection of data. These ψ-scan data were used as a calibration data-set by an empirical absorption-correction routine in the SHELXTL package of programs, a modification of the procedure of North *et al.* (1968). Absorption correction was done by assuming a pseudo-ellipsoidal shape for the crystal, and by refining the lengths and orientations of the ellipsoid semi-axes while holding $\mu \cdot R >$ constant. Absorption correction reduced the merging R of the ψ-scan data-set from 3.2 to 1.6%. Data reduction was done with a SHELXTL program, and included background and $L \cdot p$ corrections, and scaling on the standard reflection-data.

Because of the variable composition of bobfergusonite, the crystal used in the data collection was embedded in an epoxy mount and was analyzed with the electron microprobe, using the same analytical techniques as in Ercit *et al.* (1986). The composition is given in Table 2; the resulting formula given in Table 1 was used for the structure refinement.

TABLE 2. ELECTRON-MICROPROBE DATA ON BOBFERGUSONITE CRYSTAL

Na_2O	MgO	CaO	MnO	FeO	ZnO	Fe_2O_3	Al_2O_3	P_2O_5	H_2O	Total
6.8	0.4	1.1	31.6	0.3	0.4	6.7	7.5	45.1	0.3	100.2

Fe^{2+}:Fe^{3+} by Mossbauer Spectrometry, H_2O by thermogravimetry.

Structure Analysis

From the precession study, it was evident that the bobfergusonite structure is a more highly ordered derivative of the wyllieite structure. The bobfergusonite structure differs from the wyllieite structure in having a doubled *a* period and the space group $P2_1/n$, whereas the wyllieite structure obeys $P2_1/c$ (Ercit *et al.* 1986). Comparison of the symmetry of a $P2_1/c$ cell doubled along X to the symmetry of a $P2_1/n$ cell of equivalent dimensions gives two possibilities for the origin of the bobfergusonite cell with reference to a wyllieite subcell: (0,0,0)w and (½,0,0,)w, where w refers to wyllieite.

Structure analysis was done with the program X in the SHELXTL package. Scattering curves for neutral atoms from Cromer & Mann (1968) and anomalous-dispersion coefficients from Cromer & Liberman (1970) were used. A direct-methods solution of the structure uniquely gave the origin as (0,0,0)w, so that refinement was initiated with this setting. Co-ordinates for the wyllieite structure (Moore & Molin-Case 1974), transformed to comply with its $P2_1/c$ setting (Ercit *et al.* 1986), were used as starting values for the refinement. For a (0,0,0)w origin, the suppression of certain symmetry-elements by the doubled-$P2_1/c$ to $P2_1/n$ transformation splits each M-, P- and O-site, X(1a) and X(2) of the parental wyllieite structure into two non-equivalent sites; X(1b) remains unsplit but degenerates from a special to a general position [see Moore & Molin-Case (1974) for site nomenclature of the wyllieite structure]. This results in 6 M sites, 5 X sites, 6 P sites and 24 O sites in bobfergusonite. The site nomenclature adopted for bobfergusonite and its relation to the system used for wyllieite- and alluaudite-group minerals (Moore & Ito 1979, Moore 1971) are given in Table 3.

For early stages of the refinement, a wyllieite-like ordering scheme was assumed, and by using the non-genetic method of Moore & Ito (1979) for the calculation of the formula of wyllieite-group minerals, initial site-populations were assigned (Table 4). Subsequently, the total occupancy of each M and X site was refined using mean scattering-curves based on the wyllieite-like model, while constraining the temperature factors of the members of each split site to be equal.

Several cycles of refinement of the scale factor, all positional and isotropic thermal parameters and the X- and M-site occupancies gave R indices of 9.0, weighted R 8.0%. A difference Fourier map at this stage showed two large loci of residual electron-density on opposite sides of the $X1$ sites, suggesting strong anisotropic vibration for atoms of the site. Modeling the atoms of the site for anisotropic vibration reduced the R indices to $R = 6.6$, $wR = 5.7\%$. No other strong indications of anisotropic vibration

were detected at this stage; refinement of the model with the (0,0,0)*w* origin rested here.

Refinement of the model with its origin at (½,0,0)*w* began with the transformation of wyllieite coordinates, which resulted in the same number of *M*, *X*, P and O sites as the first model; however, the second model has the *X*(1a) site unsplit but degenerated to a general position, and *X*(1b) split yet remaining in special positions. The refinement procedure for the second model was the same as for the first. Refinement of the scale factor, all positional parameters, isotropic temperature-factors for all sites except the split *X*(1b) sites (strongly anisotropic) and of all *X*- and *M*-site occupancies gave $R = 8.1$, $wR = 6.8\%$, clearly inferior to the first model with $R = 6.6$, $wR = 5.7\%$. We concluded that the correct origin for bobfergusonite is at (0,0,0)*w*.

TABLE 3. SITE-CORRELATION TABLE FOR THE ALLUAUDITE STRUCTURE AND DERIVATIVES

Alluaudite	Wyllieite	Bobfergusonite
M(1)	M(1)	M1, M2
M(2)	M(2a)	M3, M4
	M(2b)	M5, M6
X(1)	X(1b)	X1
	X(1a)	X2, X3
X(2)	X(2)	X4, X5
P(1)	P(1)	P1, P2
P(2)	P(2a)	P3, P4
	P(2b)	P5, P6
O1	O(1a)	O1, O2
	O(1b)	O3, O4
O2	O(2a)	O5, O6
	O(2b)	O7, O8
O3	O(3a)	O9, O10
	O(3b)	O11, O12
O4	O(4a)	O13, O14
	O(4b)	O15, O16
O5	O(5a)	O17, O18
	O(5b)	O19, O20
O6	O(6a)	O21, O22
	O(6b)	O23, O24

TABLE 4. BOBFERGUSONITE: INITIAL AND FINAL M- AND X-SITE POPULATIONS

Site	Population
	Initial
M1, M2	1.00 Mn
M3, M4	0.02 Zn + 0.04 $Mg_{\pm}$ + 0.02 Fe^{2+} + 0.09 Fe^{3+} + 0.83 Mn
M5, M6	0.69 Al + 0.31 Fe^{3+}
X1	0.55 Mn + 0.19 Ca + 0.26 Na
X2, X3	1.00 Na
X4, X5	0.40 Na
	Final
M1	0.92(1) Mn
M2	0.91(1) Mn
M3, M4	0.82 Mn + 0.06(1) Fe^{3+} + 0.12(1) Al
M5	0.48(1) Fe^{3+} + 0.34(1) Al + 0.04 Fe^{2+} + 0.09 Mg + 0.05 Zn
M6	0.80(1) Al + 0.20(1) Fe^{3+}
X1	0.81 Mn + 0.19 Ca
X2	0.85(1) Na
X3	0.81(1) Na
X4	0.59(1) Na
X5	0.58(1) Na

In the next stage of refinement of the (0,0,0)*w* model, all atoms were modeled as vibrating anisotropically. After several cycles of refinement, the *M*- and *X*-site occupancies were critically examined for the first time. The occupancies of the following pairs of sites representing split sites of the wyllieite structure were statistically identical: *M*1 and *M*2, *M*3 and *M*4, *X*2 and *X*3, *X*4 and *X*5, indicating that no significant cation ordering exists between the members of each pair. However, the occupancies of *M*5 and *M*6 are not equivalent; the scattering from *M*5 is much stronger than that from *M*6 (significant well above the 99.8% confidence-level). On the basis of a wyllieite substructure, the main occupants of these sites are Fe and Al; therefore, the *M*5 site must be preferentially occupied by Fe, and the *M*6 site, by Al.

The model of Moore & Ito (1979) for the crystal chemistry of the wyllieite-group minerals indicates that the *M*1 and *M*2 positions of bobfergusonite should be fully occupied by Mn; however, the number of electrons at these sites is 9% lower than expected. In all refinements of wyllieite-group minerals to date (Moore & Molin-Case 1974, Zhesheng *et al.* 1983), the site in the wyllieite structure corresponding to *M*1 plus *M*2 of bobfergusonite has always been *assumed* to be fully occupied by either Mn or Fe^{2+}. On the basis of data currently available, it is not possible to determine whether the low occupancies are unique to bobfergusonite, or are typical of wyllieite-group minerals and their derivatives. Furthermore, without more data it cannot be determined whether the low occupancies are due to vacancies or to the presence of elements lighter than Mn or Fe at these sites. Refinements of two wyllieite samples and a second crystal of bobfergusonite have been initiated in order to resolve this, and other ambiguities in the crystal chemistry of the minerals. For the present time it is assumed that the *M*1 and *M*2 sites have small amounts of vacancies.

The populations of the *M*3 to *M*6, *X*1 and *X*2 sites calculated on a wyllieite-substructure model refined to full occupancy, apparently indicating that the Moore & Ito (1979) model adequately predicted the chemistry of these sites. However, bond-valence calculations for *M*3, *M*4 and *M*5 are quite nonideal. Specifically, *M*3 and *M*4 are found to have 17% more valence associated with them, and *M*5 was found to have 11% less valence associated with it than anticipated from the refined site-populations. To minimize both problems, all divalent cations except Mn^{2+} were transferred from *M*3 and *M*4 to *M*5, in exchange for trivalent Al and Fe.

The *X*2 to *X*5 sites had refined occupancies lower than 1; the corresponding sites for the wyllieite structure are typically only partly occupied, so that this behavior is not unexpected.

Taking the above points into consideration, the

following occupancy model was refined:

1. Ca: All Ca was assigned to the *X*1 site at the microprobe-determined concentration.
2. Na: All Na was assigned to the *X*2 to *X*5 sites as the sole occupant of these sites, and the total occupancy of each site was refined.
3. Zn, Mg: All Zn and Mg were assigned to the *M*5 site at their microprobe-determined concentrations, to optimize bond-valence requirements.
4. Al, Fe: The Al:Fe ratio of *M*6 was refined. Enough Al + Fe was added to fill the *M*5 site (in addition to the Zn + Mg already assigned); all remaining Al + Fe was split equally among *M*5 and *M*4. By constraining Al(R) to equal Al(T)–Al(*M*5) and Fe(R) to equal Fe(T)–Fe(*M*5), and Al(*M*3) = Al(*M*4) = Al(R)–Al(*M*5) and Fe(*M*3) = Fe(*M*4) = Fe(R)–Fe(*M*5), where Al(R) and Fe(R) are Al and Fe at *M*3 to *M*5 and Al(T) and Fe(T) are the total Al and Fe contents from results of the microprobe analysis, the *M*3- to *M*5-site Al and Fe contents were determined.
5. Mn: Mn was assigned to the *X*1 site with an occupancy of Mn = 1–Ca, and to the *M*3 and *M*4 sites with Mn = 1–(Zn + Mg + Fe + Al) for each site. All remaining Mn was assumed to reside at the *M*1 and *M*2 sites as the sole oocupant of these sites, and the total occupancies of these sites were refined.

Owing to limitations of the computer programs used in the structure refinement, random error in the microprobe data was ignored in the refinement.

For this final model, the constraint of equal temperature-factors for each member of the split sites was relaxed. The model had 372 least-squares parameters and was refined to *R* indices of 3.8, $wR = 3.4\%$. A difference-Fourier map made at this last stage had no residual electron-density maxima greater than 0.45 $e^-/Å^3$. The largest of these did not correlate with any possible proton positions; consequently, all such differences were considered as background.

The only microprobe-unconstrained compositional parameters were the Mn and Na occupancies. The refined Mn and Na contents of 4.28(1) and 2.01(2) atoms per formula unit ($Z = 4$) compare very well with microprobe-determined values of 4.21 and 2.07 atoms, an indication of the correctness of the model and the relative freedom from error of the intensity data.

The *M*5 and *M*6 sites were found to partition Al and Fe very differently. *M*5 has a refined Fe:Al ratio of 1.51, and *M*6 has an Fe:Al ratio of 0.25. The Al:Fe ordering is also reflected in the bond lengths of the *M*5 and *M*6 polyhedra; *M*5 has a mean bond-length of 2.025 Å, whereas *M*6, with its greater proportion of (smaller) Al, has a mean bond-length of 1.956 Å.

TABLE 5. BOBFERGUSONITE: POSITIONAL AND THERMAL PARAMETERS

Site	x	y	z	U(eq)
M1	0.13194(7)	0.23856(7)	-0.00190(8)	138(3)
M2	0.62989(7)	0.23753(7)	-0.00107(8)	137(3)
M3	0.29562(6)	0.14643(7)	0.72421(7)	113(2)
M4	0.79574(7)	0.14588(7)	0.72617(8)	125(2)
M5	0.46125(8)	0.16153(8)	0.27999(9)	108(3)
M6	0.96067(10)	0.16220(10)	0.27950(11)	98(4)
X1	0.24944(11)	0.00103(9)	-0.00188(11)	280(2)
X2	0	0	0	309(14)
X3	1/2	0	0	307(15)
X4	0.3734(5)	0.0169(4)	0.4972(4)	444(19)
X5	0.8738(4)	0.0166(4)	0.5004(4)	377(17)
P1	0.3816(1)	0.2183(1)	0.0033(1)	102(4)
P2	0.8826(1)	0.2152(1)	0.0067(1)	105(4)
P3	0.2013(1)	0.1141(1)	0.2578(1)	105(3)
P4	0.7041(1)	0.1134(1)	0.2598(1)	109(3)
P5	0.0597(1)	0.0957(1)	0.7384(1)	118(3)
P6	0.5588(1)	0.1000(1)	0.7400(1)	122(3)
O1	0.2980(3)	0.2105(3)	0.5460(3)	152(10)
O2	0.7979(2)	0.2081(3)	0.5458(3)	159(10)
O3	0.4655(3)	0.2182(3)	0.4503(3)	163(10)
O4	0.9637(3)	0.2141(3)	0.4457(3)	129(9)
O5	0.3290(3)	0.3698(3)	0.4182(3)	225(11)
O6	0.8267(3)	0.3666(3)	0.4151(3)	215(11)
O7	0.4426(3)	0.3508(3)	0.6102(3)	227(13)
O8	0.9444(3)	0.3475(3)	0.6048(3)	243(12)
O9	0.1125(3)	0.1720(3)	0.3151(3)	153(11)
O10	0.6180(3)	0.1743(3)	0.3182(3)	172(12)
O11	0.1343(3)	0.1522(3)	0.6592(4)	226(11)
O12	0.6357(3)	0.1544(3)	0.6613(4)	227(11)
O13	0.1098(3)	0.4102(3)	0.3729(3)	182(12)
O14	0.6116(3)	0.4133(3)	0.3713(3)	195(12)
O15	0.1714(3)	0.4022(3)	0.6215(3)	142(11)
O16	0.6709(3)	0.4005(3)	0.6197(3)	156(11)
O17	0.3011(3)	0.1851(3)	0.2765(3)	171(10)
O18	0.8056(3)	0.1819(3)	0.2753(3)	161(10)
O19	0.4591(3)	0.1710(3)	0.7370(3)	165(11)
O20	0.9596(3)	0.1642(3)	0.7351(3)	181(11)
O21	0.2776(4)	0.5080(3)	0.1785(4)	279(13)
O22	0.7773(4)	0.5072(3)	0.1757(4)	264(12)
O23	0.4651(3)	0.4846(3)	0.8149(4)	208(11)
O24	0.9717(3)	0.4900(3)	0.8150(4)	247(12)

All U's are $x10^4$.

Final positional parameters and equivalent isotropic temperature-factors are given in Table 5. The final site-populations are given in Table 4. The standard deviations reported in Table 4 are higher than those estimated from the refinement by a factor of 1–3, to reflect the higher imprecision of microprobe analysis, on which the site-occupancy refinements were based. Bond lengths are given in Table 6, and selected intrapolyhedral angles and O–O separations are given in Table 7. Observed and calculated structure-factors and anisotropic temperature-factors have been submitted to the Depository of Unpublished Data, CISTI, National Research Council of Canada, Ottawa, Canada K1A 0S2.

Description of the Structure

The bobfergusonite structure is identical to the alluaudite structure (Moore 1971) and the wyllieite structure (Moore & Molin-Case 1974) in gross topology. The bobfergusonite structure can be described as a layer structure, with alternations of strongly bonded and weakly bonded layers normal to *Y*,

TABLE 6. BOBFERGUSONITE: BOND LENGTHS (Å)

M1 - O2	2.222(4)	M2 - O1	2.241(3)	M3 - O1	2.127(4)
- O3	2.194(3)	- O4	2.215(3)	- O6	2.100(4)
- O10	2.252(4)	- O9	2.308(4)	- O11	2.097(4)
- O12	2.238(4)	- O11	2.236(4)	- O18	2.216(4)
- O14	2.352(4)	- O13	2.305(4)	- O19	2.097(3)
- O16	2.213(4)	- O15	2.231(3)	- O22	1.994(4)
< M1-O >	2.245	< M2-O >	2.256	< M3-O >	2.106
M4 - O2	2.140(4)	M5 - O3	2.002(4)	M6 - O4	1.941(4)
- O5	2.117(4)	- O8	1.921(4)	- O7	1.861(4)
- O12	2.083(4)	- O10	2.000(4)	- O9	1.934(4)
- O17	2.181(4)	- O17	2.063(4)	- O18	1.992(4)
- O20	2.096(4)	- O20	2.231(4)	- O19	2.135(4)
- O21	1.998(4)	- O24	1.932(4)	- O23	1.874(4)
< M4-O >	2.103	< M5-O >	2.025	< M6-O >	1.956
X1 - O5	2.186(4)	X2 - O5 x2	2.781(4)	X3 - O6 x2	2.835(4)
- O6	2.185(4)	- O7 x2	2.390(4)	- O8 x2	2.383(4)
- O13	2.430(4)	- O14 x2	2.393(4)	- O13 x2	2.385(4)
- O14	2.364(4)	- O16 x2	2.707(4)	- O15 x2	2.711(3)
- O15	2.150(4)	< X2-O >	2.568	< X3-O >	2.579
- O16	2.158(4)				
< X1-O >	2.246				
X4 - O1	2.692(6)	X5 - O2	2.651(6)		
- O3	2.851(6)	- O4	2.817(6)		
- O12	2.757(6)	- O11	2.740(6)		
- O21	2.560(6)	- O22	2.564(6)		
- O22	2.467(7)	- O21	2.465(7)		
- O24a	2.701(6)	- O23a	2.738(6)		
- O24b	2.502(7)	- O23b	2.480(6)		
< X4-O >	2.646	< X5-O >	2.636		
P1 - O2	1.528(4)	P2 - O1	1.528(4)	P3 - O9	1.546(4)
- O4	1.544(4)	- O3	1.538(4)	- O16	1.535(4)
- O6	1.547(4)	- O5	1.544(4)	- O17	1.545(4)
- O8	1.532(4)	- O7	1.533(4)	- O21	1.509(4)
< P1-O >	1.538	< P2-O >	1.536	< P3-O >	1.534
P4 - O10	1.543(4)	P5 - O11	1.543(4)	P6 - O12	1.548(4)
- O15	1.544(4)	- O14	1.536(4)	- O13	1.533(4)
- O18	1.544(4)	- O20	1.536(4)	- O19	1.549(4)
- O22	1.511(4)	- O23	1.525(4)	- O24	1.533(4)
< P4-O >	1.536	< P5-O >	1.535	< P6-O >	1.541

which accounts for the perfect {010} cleavage. The repeat period along Y is four layers thick.

The strongly bonded layer has a mean intralayer Pauling bond-strength of 0.6 v.u. It consists of M-cation polyhedra (distorted octahedra) and phosphate tetrahedra. The octahedra of the layer link *via* edge-sharing in *cis* configurations to form very staggered chains along [101] (Fig. 1). These chains are cross-linked by isolated phosphate tetrahedra; the P–O bonds of the tetrahedra are shown as spokes in Figure 1. In terms of M-cation ordering there are two types of chain: one type essentially consists of only Mn ($M1$ and $M4$ sites) and Fe^{3+} ($M5$ site), the other of Mn ($M2$ and $M3$ sites) and Al ($M6$ site). One-third of all phosphate tetrahedra are completely bonded within the layer; the remaining two-thirds have one P–O bond of each tetrahedron involved in cross-linking the layers of the structure.

The weakly bonded layer has a mean intralayer Pauling bond-strength of 0.2 v.u. It consists of X-cation polyhedra only (Fig. 2). The $X1$ site is mainly occupied by Mn and has an octahedral co-ordination polyhedron (stippled in Fig. 2). The $X2$ to $X5$ sites are occupied by Na. The $X2$ and $X3$ cations are 8-co-ordinate; the $X4$ and $X5$ cations are 7-co-ordinate (Na–O bonds are shown as spokes in Fig. 2). The co-ordination polyhedra of the X cations form straight chains parallel to the X axis; these chains are not cross-linked within the layer. There are two types of chain: one type consists of alternating $X1$ (Mn) and $X2$–$X3$ (Na) polyhedra in a face-sharing relationship; the other type consists only of $X4$ and $X5$ (Na) polyhedra, linked *via* edge-sharing.

The co-ordination polyhedra of the $X3$ to $M6$ and $X1$ cations are reasonably octahedral and only slightly distorted. The $M1$ and $M2$ polyhedra are very distorted octahedra, which Moore (1971) has described as bifurcated tetragonal pyramids. The co-ordination polyhedra of $X2$ and $X3$ are very distorted cubes, the irregularity arising from two anomalously large, symmetrically equivalent edges in each polyhedron (O5–O14 for $X2$ and O6–O13 for $X3$, Table 7). The co-ordination polyhedra of $X4$ and $X5$ are diminished gable disphenoids.

Cation Ordering

The cation-ordering scheme of the bobfergusonite structure is very similar to that of the wyllieite structure. Complete disorder of cations exists between the pseudosymmetrical pairs of sites $M1$–$M2$, $M3$–$M4$, $X2$–$X3$ and $X4$–$X5$; however, significant Al *versus* Fe^{3+} ($+Fe^{2+}+Mg+Zn$) ordering occurs between the $M5$ and $M6$ sites, which is not permitted in the wyllieite structure. $M6$ shows a strong preference for Al; $M5$ prefers the larger Fe^{3+} and lower-charged cations such as Fe^{2+}, Zn and Mg.

The validity of using a wyllieite substructure as a starting point for determining the ordering scheme of cations in bobfergusonite was proven by the low R-indices and by the good agreement between the Mn^{2+} and Na^{+} contents from the structure refinement and microprobe-determined values. However, mean polyhedral bond-lengths and bond-valence sums can also be used to assess the validity of the model. In Table 8, a comparison is made between the observed mean polyhedral bond-lengths and values calculated from Shannon (1976a), using the final site-populations of Table 4. In general, agreement between the observed and calculated mean bond-lengths is reasonable. Differences increase with increasing bond-length; this is to be expected, as the weaker the average bond-valence to a cation, the more easily the mean bond-length is perturbed from ideality by such factors as polyhedron distortion. With only 60% occupancy of the $X4$ and $X5$ sites by Na, there is a significant increase in the mean bond-length over that expected; this effect has been well documented in Li compounds (Shannon 1976b).

Bond valences (Brown 1981) may also be used to assess the validity of the results. Because of the large number of sites, only bond-valence sums to the sites are presented here (Table 9). The following section summarizes the results:

1. $M1$, $M2$: The bond-valence sums are 11–14% lower than expected for a model with 91–92% occupancy of Mn at these sites, which may indicate the presence of minor Na.

TABLE 7. BOBFERGUSONITE: SELECTED ANGLES (°), O-O SEPARATIONS (Å)

M1 Polyhedron		M2 Polyhedron		M3 Polyhedron	
O2-O10	91.8(4), 3.213(6)	O1-O9	92.6(1), 3.291(6)	O1-O11	78.4(1), 2.669(5)
-O12	73.0(1), 2.652(6)	-O11	73.2(1), 2.669(5)	-O18	82.2(2), 2.856(5)
-O14	114.5(1), 3.846(7)	-O13	113.7(1), 3.807(7)	-O19	83.0(1), 2.799(5)
-O16	87.5(1), 3.068(5)	-O15	86.5(1), 3.063(5)	-O22	97.4(2), 3.099(6)
O3-O10	72.7(1), 2.634(5)	O4-O9	69.5(1), 2.580(5)	O6-O11	113.6(2), 3.511(7)
-O12	88.2(1), 3.084(6)	-O11	88.3(1), 3.100(6)	-O18	79.8(1), 2.769(5)
-O14	91.4(1), 3.255(6)	-O13	91.6(1), 3.241(6)	-O19	83.2(1), 2.788(6)
-O16	118.4(1), 3.786(7)	-O15	121.4(1), 3.878(7)	-O22	101.3(2), 3.168(6)
O10-O12	114.3(1), 3.773(7)	O9-O11	112.6(1), 3.780(7)	O11-O18	94.4(1), 3.165(6)
-O14	82.8(1), 3.046(5)	-O13	82.5(1), 3.044(5)	-O22	82.2(2), 2.693(5)
O12-O16	90.0(1), 3.148(6)	O11-O15	91.3(1), 3.193(6)	O18-O19	79.4(1), 2.759(5)
O14-O16	74.2(1), 2.755(5)	O13-O15	74.9(1), 2.759(5)	O19-O22	103.9(2), 3.226(6)
<O-M1-O>	91.6	<O-M2-O>	91.5	<O-M3-O>	89.9
<O-O>	3.188	<O-O>	3.200	<O-O>	2.958

M4 Polyhedron		M5 Polyhedron		M6 Polyhedron	
O2-O12	77.8(1), 2.652(6)	O3-O10	82.3(2), 2.634(5)	O4-O9	83.5(2), 2.580(5)
-O17	83.2(1), 2.870(5)	-O17	82.9(1), 2.692(5)	-O18	83.3(1), 2.613(4)
-O20	82.8(1), 2.802(5)	-O20	82.1(1), 2.785(5)	-O19	83.1(1), 2.708(5)
-O21	96.8(2), 3.096(6)	-O24	99.5(2), 3.004(6)	-O23	97.6(2), 2.872(5)
O5-O12	114.5(2), 3.531(7)	O8-O10	101.5(2), 3.037(6)	O7-O9	101.8(2), 2.945(6)
-O17	80.7(1), 2.793(5)	-O17	90.2(2), 2.825(6)	-O18	89.4(2), 2.712(6)
-O20	83.6(2), 2.809(6)	-O20	80.6(2), 2.696(6)	-O19	82.4(2), 2.641(6)
-O21	100.2(2), 3.157(6)	-O24	98.1(2), 2.909(6)	-O23	96.9(2), 2.796(6)
O12-O17	92.1(1), 3.069(6)	O10-O20	87.2(1), 2.922(5)	O9-O19	88.0(2), 2.830(5)
-O21	83.2(2), 2.711(6)	-O24	89.7(2), 2.773(6)	-O23	90.9(2), 2.715(5)
O17-O20	83.3(1), 2.843(5)	O17-O20	82.8(1), 2.843(5)	O18-O19	83.8(2), 2.758(5)
O20-O21	101.5(2), 3.172(6)	-O24	100.8(2), 3.079(6)	-O23	97.5(2), 2.907(5)
<O-M4-O>	90.0	<O-M5-O>	90.0	<O-M6-O>	90.0
<O-O>	2.958	<O-O>	2.850	<O-O>	2.756

X1 Polyhedron		X2 Polyhedron		X3 Polyhedron	
O5-O13	75.4(1), 2.828(5)	O5-O7 x2	124.7(1)	O6-O8 x2	125.3(1)
-O14	104.0(1), 3.587(7)	-O7 x2	55.3(1), 2.425(5)	-O8 x2	54.7(1), 2.431(5)
-O15	96.0(1), 3.223(6)	-O14 x2	87.4(1)	-O13 x2	88.8(1)
-O16	83.7(2), 2.898(5)	-O14 x2	92.6(1), 3.750(7)	-O13 x2	91.2(1), 3.744(7)
O6-O13	105.0(1), 3.665(7)	-O16 x2	116.3(1)	-O15 x2	116.6(1)
-O14	75.6(1), 2.792(5)	-O16 x2	63.7(1), 2.898(5)	-O15 x2	63.4(1), 2.916(5)
-O15	84.5(2), 2.916(5)	O7-O14 x2	101.1(1)	O8-O13 x2	98.2(1)
-O16	95.7(2), 3.221(6)	-O14 x2	78.9(1), 3.039(6)	-O13 x2	81.8(1), 3.121(6)
O13-O15	73.8(1), 2.759(5)	-O16 x2	109.0(1)	-O15 x2	109.2(1)
-O16	105.6(1), 3.659(7)	-O16 x2	71.0(1), 2.971(6)	-O15 x2	70.8(1), 2.963(6)
O14-O15	105.6(1), 3.598(7)	O14-O16 x2	115.0(1)	O13-O15 x2	114.8(1)
-O16	74.9(1), 2.755(5)	-O16 x2	65.0(1), 2.755(5)	-O15 x2	65.2(1), 2.759(5)
<O-X1-O>	90.0	<O-X2-O>	90.0	<O-X3-O>	90.0
<O-O>	3.158	<O-O>	2.973	<O-O>	2.989

X4 Polyhedron		X5 Polyhedron	
O1 -O3	53.7(1), 2.504(5)	O2 -O4	54.5(1), 2.510(5)
-O21	86.3(2), 3.587(7)	-O22	85.8(2), 3.550(7)
-O22	73.9(2), 3.099(6)	-O21	74.4(2), 3.096(6)
-O24a	101.9(2)	-O23a	104.4(2)
-O24b	114.9(2)	-O23b	112.5(2)
O3 -O21	100.9(2)	O4 -O22	99.6(2)
-O22	120.7(2)	-O21	122.5(2)
-O24a	88.3(2), 3.867(7)	-O23a	89.9(2), 3.926(7)
-O24b	67.9(2), 3.004(6)	-O23b	65.3(2), 2.872(5)
O12-O21	61.2(2), 2.711(6)	O11-O22	60.9(2), 2.693(5)
-O22	115.2(2)	-O21	115.7(2)
-O24a	111.0(2)	-O23a	109.3(2)
-O24b	56.6(2), 2.501(6)	-O23b	56.5(2), 2.483(5)
O21-O22	101.3(2), 3.888(7)	O22-O21	101.3(2), 3.888(7)
-O24b	78.2(2), 3.194(6)	-O23b	76.2(2), 3.114(6)
O22-O24a	76.3(2), 3.197(6)	O21-O23a	78.0(2), 3.280(6)
O24a-O24b	102.7(2), 4.064(7)	O23a-O23b	103.1(2), 4.089(7)
<O-X4-O>	88.9	<O-X5-O>	88.8
<O-O>	3.238	<O-O>	3.227

P1 Tetrahedron		P2 Tetrahedron		P3 Tetrahedron	
O2-O4	109.6(2), 2.510(5)	O1-O3	109.5(2), 2.504(5)	O9-O16	110.8(2), 2.536(5)
-O6	109.0(2), 2.504(5)	-O5	108.9(2), 2.498(5)	-O17	108.2(2), 2.503(5)
-O8	114.8(2), 2.579(5)	-O7	114.9(2), 2.580(5)	-O21	108.5(2), 2.479(6)
O4-O6	113.2(2), 2.580(5)	O3-O5	112.9(2), 2.568(5)	O16-O17	107.7(2), 2.487(5)
-O8	105.9(2), 2.456(5)	-O7	106.7(2), 2.463(6)	-O21	111.5(2), 2.516(6)
O6-O8	104.3(2), 2.431(5)	O5-O7	104.0(2), 2.425(5)	O17-O21	110.2(2), 2.505(6)
<O-P1-O>	109.5	<O-P2-O>	109.5	<O-P3-O>	109.5
<O-O>	2.510	<O-O>	2.506	<O-O>	2.504

P4 Tetrahedron		P5 Tetrahedron		P6 Tetrahedron	
O10-O15	110.9(2), 2.542(5)	O11-O14	110.6(2), 2.531(6)	O12-O13	110.5(2), 2.531(6)
-O18	108.3(2), 2.502(5)	-O20	107.7(2), 2.485(6)	-O19	108.4(2), 2.511(6)
-O22	108.3(2), 2.475(5)	-O23	108.1(2), 2.483(5)	-O24	108.6(2), 2.501(6)
O15-O18	107.4(2), 2.488(5)	O14-O20	108.8(2), 2.497(5)	O13-O19	108.5(2), 2.502(5)
-O22	111.2(2), 2.520(5)	-O23	110.2(2), 2.510(5)	-O24	111.1(2), 2.529(5)
O18-O22	110.7(2), 2.514(5)	O20-O23	111.4(2), 2.528(6)	O19-O24	109.7(2), 2.520(6)
<O-P4-O>	109.5	<O-P5-O>	109.5	<O-P6-O>	109.5
<O-O>	2.507	<O-O>	2.506	<O-O>	2.516

2. *M*3–*M*5: As mentioned earlier, the starting populations for these sites (Table 4) gave quite nonideal results, necessitating a transfer of Zn, Mg and Fe^{2+} from *M*3 and *M*4 to *M*5, in return for Al and Fe^{3+}. This reduced the observed *versus* expected bond-valence discrepancies from +17% to +11% for *M*3 and *M*4, and from −11% to −7% for *M*5.
3. *M*6, *X*1–*X*3: The bond-valence sums to these sites are well within expectations.
4. *X*4, *X*5: The sums to these sites are low by approximately 20% with respect to a model with 58–59% occupancy of these sites, a reflection of the bond-length perturbations with low site-occupancy discussed earlier.
5. P1–P6: All sums to the P sites are within expectations.
6. O1–O24: All bond-valence sums to the O sites are within expectations. There is no strong indication of any preferred sites for O-for-OH substitution.

The observed cation-ordering scheme for bobfergusonite indicates that its structural formula is:

$$[X5_4X4_4][X3_2X2_2]X1_4$$
$$[M1_4M2_4][M3_4M4_4]M5_4M6_4(PO_4)_{24}$$

where, ideally, *X*2–*X*5 = Na, *X*1, *M*1–*M*4 = Mn, *M*5 = Fe^{3+}, and *M*6 = Al. Full occupancy of all sites by the cations indicated would give an excess charge of +4 per 24(PO_4); however, the *X*4 and *X*5 sites are only half-occupied by Na, thus neutralizing the excess positive charge. The simplified ideal formula is $\square Na_2Mn_5Fe^{3+}Al(PO_4)_6$ ($Z = 4$).

Ordering among the *X*-cation sites of the bobfergusonite structure is identical to that in the wyllieite structure, although a potential for higher degrees of

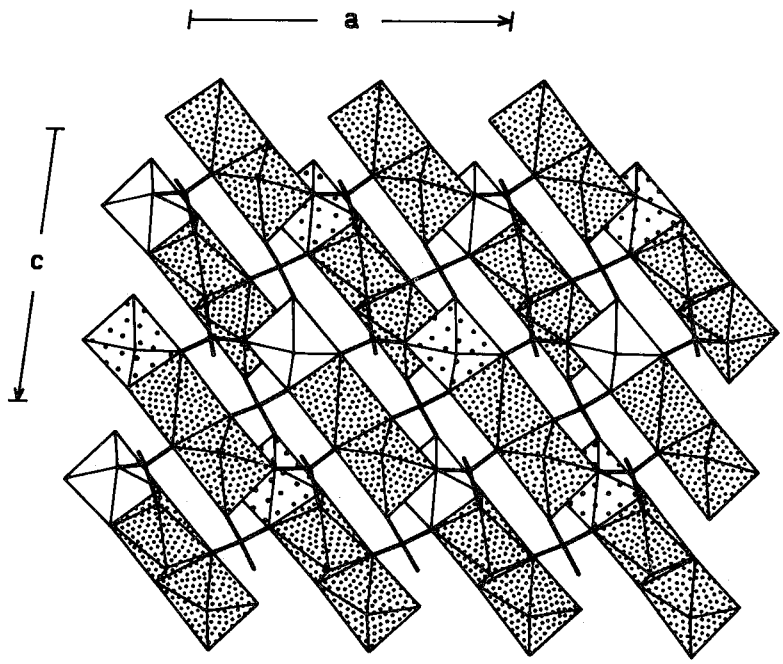

FIG. 1. The strongly bonded layer of the bobfergusonite structure. *M*-cation polyhedra link *via* edge-sharing to form staggered chains parallel to [101]. Key to the polyhedra: Mn, densely stippled; Fe^{3+}, lightly stippled; Al, unshaded. P–O bonds of PO_4 tetrahedra at the same level as, to slightly above, these octahedral chains are shown as spokes (bold rule).

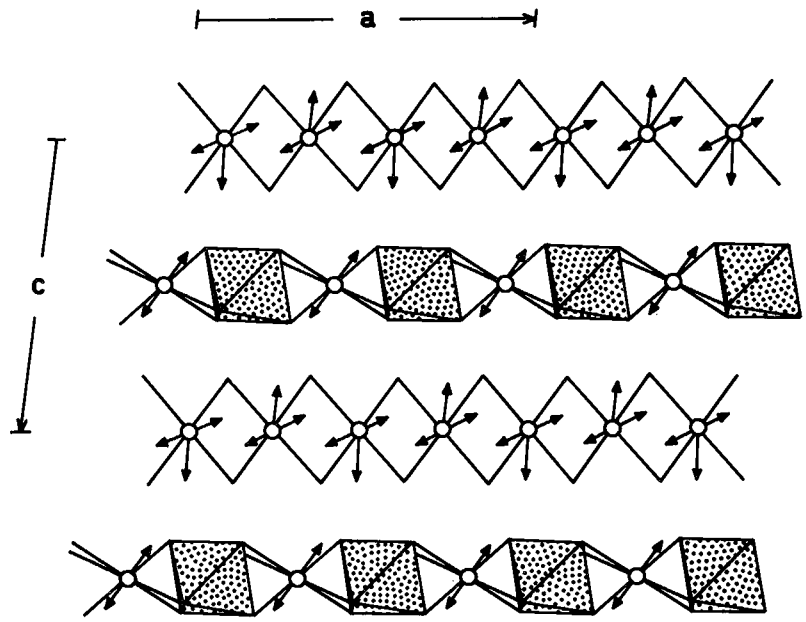

FIG. 2. The weakly bonded layer of the bobfergusonite structure. The *X*1 polyhedron is an octahedron, and is represented in dense stippling, to signify occupancy by Mn. The *X*2–*X*5 sites are occupied by Na; Na–O bonds of their co-ordination polyhedra are represented as spokes. Spokes without arrows denote bonding within the layer; spokes with arrows denote bonds that serve to link adjacent weakly and strongly bonded layers.

TABLE 8. BOBFERGUSONITE: MEAN M- AND X-SITE BOND LENGTHS (Å)

Bond	Obs.	Calc.	Bond	Obs.	Calc.
< M1-O >	2.245	2.20	< X1-O >	2.246	2.24
< M2-O >	2.256	2.20	< X2-O >	2.568	2.55
< M3-O >	2.106	2.16	< X3-O >	2.578	2.55
< M4-O >	2.103	2.16	< X4-O >*	2.646	2.50
< M5-O >	2.025	1.99	< X5-O >*	2.636	2.50
< M6-O >	1.956	1.93			

Bond lengths calculated from the ionic radii of Shannon (1976a), using the site populations of Table 4.

* only 60% occupied.

TABLE 9. BOBFERGUSONITE: BOND VALENCE SUMS (v.u.)

Site	Calc.	Exp.	Site	Calc.	Exp.
M1	1.61	1.8	O1	1.99	2
M2	1.54	1.8	O2	2.00	2
M3	2.42	2.2	O3	2.06	2
M4	2.44	2.2	O4	2.05	2
M5	2.65	2.8	O5	2.05	2
M6	2.90	3	O6	2.05	2
			O7	2.04	2
			O8	2.01	2
X1	1.95	2	O9	1.95	2
X2	0.94	0.85	O10	1.96	2
X3	0.89	0.81	O11	1.97	2
X4	0.46	0.58	O12	1.96	2
X5	0.47	0.59	O13	1.86	2
			O14	1.86	2
			O15	1.98	2
P1	5.03	5	O16	2.02	2
P2	5.06	5	O17	1.95	2
P3	5.09	5	O18	1.96	2
P4	5.06	5	O19	1.91	2
P5	5.07	5	O20	1.90	2
P6	4.99	5	O21	2.06	2
			O22	2.05	2
			O23	2.04	2
			O24	1.95	2

Bond valences calculated from Brown (1981). Expected bond-valences from Table 4 site populations.

order exists. The alluaudite structure is less ordered than these; specifically, intrachain ordering of *X* cations is not shown (Moore & Molin-Case 1974).

Figure 3 illustrates idealized Al^{3+} – Fe^{3+} – M^{2+} cation ordering in the *M*-cation octahedral chains of the alluaudite, wyllieite and bobfergusonite structures. The *M*-cation chains of the alluaudite structure (Fig. 3a) are host to Fe^{3+} and a wide range of divalent cations, but Al is present only in subordinate quantities, and plays a crystallographically indistinct role from Fe^{3+} . Consequently, Al is not a variable in the ordering scheme of the alluaudite structure. The alluaudite structure has only two crystallographically distinct *M*-cation sites (Table 3); Fe^{3+} – M^{2+} cation order ranges from complete M^{2+}-cation disorder over both sites (top of Fig. 3a) to complete Fe^{3+} – M^{2+} order, *i.e.*, with all M^{2+} at one site and all Fe^{3+} at the other (bottom of Fig. 3a).

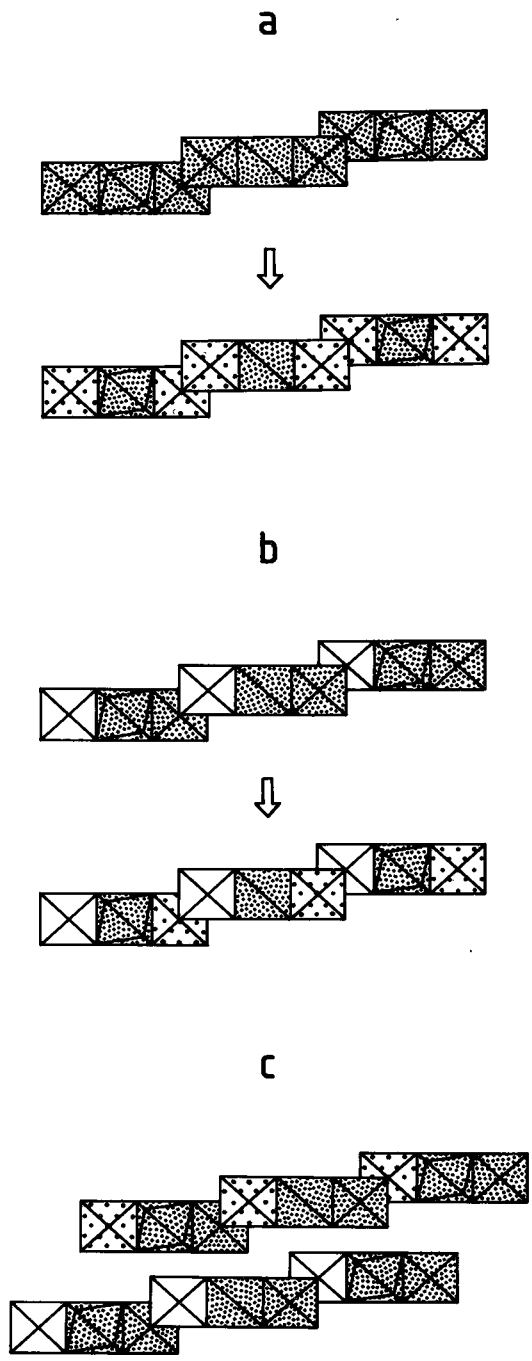

FIG. 3. Al – Fe^{3+} – M^{2+} cation ordering in the alluaudite (*a*), wyllieite (*b*), and bobfergusonite (*c*) structure-types. Polyhedron shading is as in Figure 1, except that the use of dense stippling is extended to represent polyhedra of any M^{2+} cation.

Wyllieite-group minerals are typified by dramatically higher Al-contents than alluaudite-group minerals (Moore & Ito 1979); consequently, Al takes a crystallographically distinct role from that of Fe^{3+} in the wyllieite structure. The wyllieite structure has three crystallographically distinct *M*-cation sites. The most disordered samples of wyllieite should have Al in one *M* site [*M*(2b)], and all M^{2+} disordered over the other two sites [*M*(2a) and *M*(1); top of Fig. 3b]. The most highly ordered samples of wyllieite have Al, Fe^{3+} and Fe^{2+} in separate *M* sites (bottom of Fig. 3b). As with the alluaudite structure, *M*-cation ordering produces only one crystallographically distinct type of chain for each structure.

Nonideal cation-ordering in wyllieite results in minor alluaudite-structure character. Specifically, alluaudite-like site mixing in wyllieite-group minerals results in the presence of minor Al at the Fe^{3+} site [*M*(2)], and of minor Fe^{3+} and M^{2+} at the Al site [*M*(2b)], as with type ferrowyllieite (Moore & Molin-Case 1974). None of the wyllieite samples described in Moore & Ito (1979) show ideal *M* cation order of the wyllieite structure; all have a slight to significant, but not dominant, alluaudite-structure character.

The bobfergusonite structure (Fig. 3c) has Al taking a crystallographically distinct role from that of Fe^{3+}, but unlike the wyllieite structure, additional ordering results in nonequivalence of adjacent *M*-cation chains. The bobfergusonite structure has six crystallographically distinct sites; however, only four of these sites are chemically distinct in the refined structure. The refined structure has two crystallographically distinct types of *M*-cation chains. Ideally one such chain consists of Al at one *M* site, with M^{2+} disordered over its two remaining *M* sites; the other type of chain has a similar pattern of ordering, but has Fe^{3+} in place of Al. However, the refined structure has a minor wyllieite-structure or alluaudite-structure character. Wyllieite-like site mixing should result in exchange of Al and Fe^{3+} between *M*5 and *M*6; alluaudite-like site mixing should result in Al and Fe^{3+} exchange between *M*5–*M*6 and *M*3–*M*4. Although the data suggest that alluaudite-like site mixing is prevalent, more bobfergusonite refinements are needed in order to be conclusive. The implication from Moore & Ito (1979) is that postcrystallization oxidation of wyllieite-group minerals and of bobfergusonite may be partly responsible for nonideal cation ordering in the two types of structure; additional structure-refinements of wyllieite and bobfergusonite will be done to test this model.

Acknowledgements

The authors would like to thank C.A. McCammon, formerly of the Department of Physics, University of Manitoba for collecting the Mössbauer spectra, and R.A. Ramik of the Royal Ontario Museum for the TG analysis. Financial support for this work was provided by Natural Sciences and Engineering Research Council of Canada operating grants to PČ and FCH, and by the Canada–Manitoba Interim Agreement on Mineral Development, 1982–1984.

References

Brown, I.D. (1981): The bond-valence method: an empirical approach to chemical structure and bonding. *In* Structure and Bonding in Crystals II (M. O'Keeffe & A. Navrotsky, eds.). Academic Press, New York.

Cromer, D.T. & Liberman, D. (1970): Relativistic calculation of anomalous scattering factors for X-rays. *J. Chem. Phys.* **53**, 1891-1898.

_____ & Mann, J. (1968): X-ray scattering factors computed from numerical Hartree–Fock wave functions. *Acta Cryst.* **A24**, 321-324.

Ercit, T.S., Anderson, A.J., Černý, P. & Hawthorne, F.C. (1986): Bobfergusonite: a new primary phosphate mineral from Cross Lake, Manitoba. *Can. Mineral.* **24**, 599-604.

Moore, P.B. (1971): Crystal chemistry of the alluaudite structure type: contribution to the paragenesis of pegmatite phosphate giant crystals. *Amer. Mineral.* **56**, 1955-1975.

_____ & Ito, J. (1979): Alluaudites, wyllieites, arrojadites: crystal chemistry and nomenclature. *Mineral. Mag.* **43**, 227-235.

_____ & Molin-Case, J. (1974): Contribution to pegmatite phosphate giant crystal paragenesis. II. The crystal chemistry of wyllieite, $Na_2Fe^{2+}{}_2Al[PO_4]_3$, a primary phase. *Amer. Mineral.* **59**, 280-290.

North, A.C.T., Phillips, D.C. & Mathews, F.S. (1968): A semi-empirical method of absorption correction. *Acta Cryst.* **A24**, 351-359.

Shannon, R.D. (1976a): Revised effective ionic radii and systematic studies of interatomic distances in halides and chalcogenides. *Acta Cryst.* **A32**, 751-767.

_____ (1976b): Systematic studies of interatomic distances in oxides. *In* The Physics and Chemistry of Minerals and Rocks (R.G.J. Strens, ed.). J. Wiley & Sons, London.

Zhesheng, Ma, Nicheng, Shi & Zhizhong, Peng (1983): Crystal structure of a new phosphatic mineral – qingheiite. *Scientia Sinica* **B26**, 876-884.

Received October 23, 1985, revised manuscript accepted September 17, 1986.